

**Vibrational Spectra, Vibrational Analysis and Stereochemistries of the
Pentacoordinate Molecules $\text{SiCl}_3\text{X} \cdot \text{N}(\text{CH}_3)_3$ and $\text{SiCl}_3\text{X} \cdot \text{N}(\text{CD}_3)_3$
where X = H, F, Br, or I**

D. BOAL AND G. A. OZIN¹

Lash Miller Chemistry Laboratory and Erindale College, University of Toronto, Toronto, Ontario

Received June 27, 1972

The thermally unstable compounds $\text{SiCl}_3\text{X} \cdot \text{N}(\text{CH}_3)_3$ and $\text{SiCl}_3\text{X} \cdot \text{N}(\text{CD}_3)_3$, where X = H, F, Br, or I are studied at -196°C by infrared and Raman spectroscopy. The data are compatible with molecular five coordinate compounds having a trigonal bipyramidal stereochemistry with the ligand trimethylamine always in the axial position. Using the vibrational data and normal coordinate analyses in both the C_s and C_{3v} configurations, X is suggested to be equatorial for H and F and axial for Br and I. The factors influencing the position of X in the compounds are discussed.

Les composés thermiquement instables $\text{SiCl}_3\text{X} \cdot \text{N}(\text{CH}_3)_3$ et $\text{SiCl}_3\text{X} \cdot \text{N}(\text{CD}_3)_3$ où X = H, F, Br, ou I ont été étudiés à -190°C par spectroscopie infrarouge et Raman. Les résultats peuvent être attribués à des composés moléculaires de coordination cinq (5) possédant une stéréochimie bipyramidale trigonale avec le ligand triméthylamine toujours en position axiale. En utilisant les données vibrationnelles et les analyses en coordonnées normales pour les configurations C_s et C_{3v} , on peut supposer que X est équatorial pour H et F, axial pour Br et I. Les facteurs influençant la position de X dans les composés sont discutés.
[Traduit par le journal]

Can. J. Chem., 51, 609 (1973)

Introduction

Stereochemical information for the compounds $\text{SiCl}_3\text{X} \cdot \text{NMe}_3$ where X = H, F, Br, or I have not previously been reported although the existence of the hydride and fluoride has been known for some time (1, 2). The compounds are found to be stable at -196°C , yet completely dissociated into free halide and amine at room temperature. Dissociation pressure measurements have been reported for the series $\text{SiCl}_n\text{H}_{4-n} \cdot \text{NMe}_3$ and $\text{SiCl}_n\text{F}_{4-n} \cdot \text{NMe}_3$ where the results indicated the influence of steric and electronegativity effects on the stability order of the molecules (3, 4). With recent improvements in low temperature infrared and Raman techniques, there has been renewed interest in vibrational and structural studies of unstable co-ordination compounds.

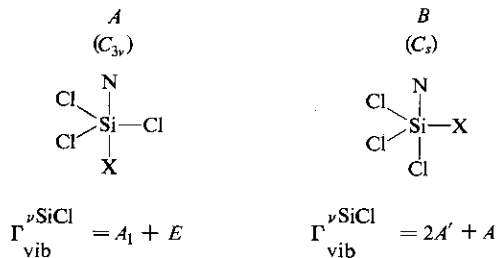
In an attempt to study these complexes, it was assumed that the basic shape at silicon was trigonal bipyramidal, with the trimethylamine ligand lying axially. Vibrational and single crystal Raman spectra and x-ray data (5, 6) for the complexes $\text{MX}_4 \cdot \text{NMe}_3$ (M = Si, Ge, or Sn and X = F or Cl), $\text{MX}_3 \cdot 2\text{NMe}_3$ (M = Al, Ga, or In and X = H, Cl, or Br) and $\text{MX}_3 \cdot \text{NMe}_3$ (M = P or As and X = Cl or Br) have been reported and the evidence is overwhelmingly in

favor of the amine lying axially. Assuming this, the question is then whether the X atom will reside in the equatorial or axial position for the series $\text{SiCl}_3\text{X} \cdot \text{NMe}_3$. An argument has been put forward (7) that for trigonal bipyramidal molecules, the most electropositive atom will lie in the equatorial plane and hence one would expect to find Cl, F, Cl, and Cl in the axial positions for the series X = H, F, Br, and I. If the trimethylamine ligand were sterically bulky enough to crowd the atoms in the equatorial plane, then one might expect to find Cl, Cl, Br, and I for the same series. A third hypothesis based on molecular orbital theory is put forward in this paper, and leads to the same predictions as the steric argument. By examining the vibrational spectra of the complexes and their perdeutero analogs, it was found that the axial atoms were Cl, Cl, Br, and I for the series X = H, F, Br, and I.

Before going into detail, it is worthwhile to discuss the spectrum of the parent molecule $\text{SiCl}_4 \cdot \text{NMe}_3$ (8, 9), which has been reported to have C_{3v} symmetry with the trimethylamine ligand in the axial position. Its spectrum is very close to that of $\text{GeCl}_4 \cdot \text{NMe}_3$ which has been shown from single crystal Raman (9) and X-ray (10) data to have the above structure. The vibrational spectrum is easily divided into ligand and acceptor modes (9), the former experiencing

¹To whom correspondence should be addressed.

50–80 cm^{-1} shifts upon deuteration of the trimethylamine. The Si—Cl stretching modes are easily discernible because of their much smaller shifts upon deuteration. The asymmetric E mode of the equatorial chlorines is found at 582 cm^{-1} (high frequency), being strong in the infrared and weak in the Raman. The symmetrical A_1 of the equatorial chlorines comes at low frequency, 361 cm^{-1} , and is strong in the Raman. This low frequency (300–380 cm^{-1}) mode is common for light central metal atoms, for example, aluminum, silicon, and phosphorus. The other A_1 mode involves the axial silicon–chlorine stretch. This mode, because it contains motion of the silicon atom (whereas the other A_1 does not), is expected to come at higher frequencies, and indeed is observed at 385 cm^{-1} . It is significant to note that in the vibrational analysis of this complex, the axial stretching force constant was found to have one half the value of the equatorial one. In addition, the crystal structure of $\text{AsCl}_3 \cdot \text{NMe}_3$ (12) (which is based on a trigonal bipyramid with an equatorial lone pair) and $\text{GeCl}_4 \cdot \text{NMe}_3$ (10) shows the axial bond to be significantly longer than the equatorial one. The trimethylamine complex with SiCl_3X can then have two possible stereochemistries



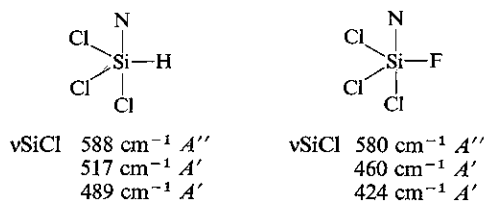
In configuration A , one would expect to find only one strong Raman peak in the Si—Cl stretching region due to the A_1 mode at about 370 cm^{-1} , as with monomeric AlCl_3 (11) (371 cm^{-1}). In B , however, there should be an A' mode due to the axial stretch above 380 cm^{-1} , and another A' mode having frequency greater than 400 cm^{-1} (the high frequency caused by both the motion of the silicon atom and the higher equatorial force constant compared to the axial one).

On the basis of the silicon–chlorine symmetric stretches, the stereochemistries were assigned. The perdeutero analogs were prepared to distin-

guish donor from acceptor modes, and normal coordinate calculations on each possible configuration were carried out.

$\text{SiCl}_3\text{H} \cdot \text{NMe}_3$ and $\text{SiCl}_3\text{F} \cdot \text{NMe}_3$

The spectra, observed and calculated, are tabulated in Tables 1 and 2. Both molecules show no silicon–chlorine stretching frequencies below 400 cm^{-1} , but rather two *high* frequency modes in the Raman. This strongly favors the hydrogen and fluorine atoms occupying the equatorial positions.



No serious attempt is made to assign the region under 300 cm^{-1} as the spectrum is far too complex (also indicating C_s symmetry). The low frequency calculated for the silicon–chlorine axial stretch in $\text{SiCl}_3\text{H} \cdot \text{NMe}_3$ is due simply because of the very low force constant. If this force constant was raised to 3/4 of the equatorial, one obtains a frequency in the region observed. The calculations for a C_{3v} configuration are shown in Table 3. The Si—Cl stretching frequency calculated is significantly lower than that observed, and in order to raise this calculated value to even 470 cm^{-1} , a force constant of about double the SiCl_4 value must be employed. Clearly this is unacceptable since the SiCl_4 force constant should decrease, not increase, upon coordination. The C_{3v} model is also unable to explain the presence of two high frequency SiCl stretching modes; it predicts only one.

$\text{SiCl}_3\text{Br} \cdot \text{NMe}_3$ and $\text{SiCl}_3\text{I} \cdot \text{NMe}_3$

The spectra for these complexes are very different from the previous two (Tables 4 and 5). Both show only one strong band in the *low* frequency silicon–chlorine stretching region at about 370 cm^{-1} , and no acceptor modes between 400–550 cm^{-1} .

Evidence against an ionic formulation [$\text{SiCl}_3 \cdot \text{NMe}_3^+$] [X^-] for the bromide and iodide adducts stems from three observations: (i) the observed νSiBr and νSiI (382 and 332 cm^{-1} respectively) stretching modes are far too high and indicate normal covalently bonded halogen; (ii) the a_1 and e νSiCl frequencies for a “pyrami-

TABLE 1. Vibrational spectrum of $\text{SiCl}_3\text{H.NMe}_3^*$

$\text{SiCl}_3\text{H.N(CH}_3)_3^\dagger$ Raman (solid at -196°C)	$\text{SiCl}_3\text{H.N(CD}_3)_3^\dagger$ Raman (solid at -196°C)	Calculated ‡ $\text{SiCl}_3\text{H.N(CH}_3)_3$	Approximate description of mode
588vww	—	593	A'' $\nu\text{SiCl}_{\text{eq}}$
517s br	522mw	508 {	A' $\nu\text{SiCl}_{\text{eq}}$
		545 }	A' δNMe_3
489ms	492s	434	A' $\nu\text{SiCl}_{\text{ax}}$
435m	434w	430	$A' + A''$ δNMe_3
423w sh	378w	425	A' $\delta\text{N(CD}_3)_3$
	331m	396	A' $\delta\text{N(CD}_3)_3$
346mw	296mw		A'' $\delta\text{N(CD}_3)_3$
322mw			
305w			
280mw	268mw		
	252mw		
252w sh			
243mw	222ms		
226ms	217ms		
213ms			
	192mw		
154w	148w		
113m	107m		

Frequencies are reported in units of cm^{-1} . † Metal-halogen skeletal stretching modes are in italics. ‡ Only the Si—Cl stretching and NMe_3 deformation region is shown in the calculations.TABLE 2. Vibrational spectrum of $\text{SiCl}_3\text{F.NMe}_3^$

$\text{SiCl}_3\text{F.N(CH}_3)_3^\dagger$		$\text{SiCl}_3\text{F.N(CD}_3)_3^\dagger$	Calculated ‡ $\text{SiCl}_3\text{F.N(CH}_3)_3$	Approximate description of mode
Infrared	Raman	Raman		
857s	868w	869mw	984	A' νSiF
578vs	580vww	582vw	648	A'' $\nu\text{SiCl}_{\text{eq}}$
538m	535mw		581	A' δNMe_3
460vww	460mw	464ms	469	A' $\nu\text{SiCl}_{\text{eq}}$
	442w		430	A'' $\delta\text{NMe}_3 + A'$ $\delta\text{N(CD}_3)_3$
	424vs	430vs	429	A' $\delta\text{N(CD}_3)_3$
390s		392mw	434	A' $\nu\text{SiCl}_{\text{ax}}$
	378w	379w sh	396	A' $\delta\text{N(CD}_3)_3$
360s	330mw	362vw		
283w		302w br		
	268w			
254w	250mw	255m		
235w	236mw			
	225mw	223ms br		

*Frequencies are reported in units of cm^{-1} . † Metal-halogen skeletal stretching modes are in italics. ‡ Because of C_2 symmetry, the region below 400 cm^{-1} is very complex and is therefore not assigned.

TABLE 3. Calculated frequencies for $\text{SiCl}_3\text{X.NMe}_3$ (X=H and F), C_{3v} symmetry*

$\text{SiCl}_3\text{H.NMe}_3$			$\text{SiCl}_3\text{F.NMe}_3$		
H9	Approximate description of mode	D9	H9	Approximate description of mode	D9
612	<i>E</i> νSiCl	612	643	<i>E</i> νSiCl	643
563	<i>A</i> ₁ δNMe_3	532	545	<i>A</i> ₁ δNMe_3	515
430	<i>E</i> δNMe_3	396	430	<i>E</i> δNMe_3	396
376	<i>A</i> ₁ νSiCl	376	378	<i>A</i> ₁ νSiCl	378
334	<i>A</i> ₁ νSiN	328			
			269	<i>A</i> ₁ νSiN	263
247	<i>E</i> $\rho_r\text{NMe}_3$	231	249	<i>E</i> $\rho_r\text{NMe}_3$	236
			218	<i>E</i> δFSiCl	215
161	<i>E</i> $\delta\text{SiCl i.p.}$	160			
			156	<i>E</i> $\delta\text{SiCl i.p.}$	155
135	<i>A</i> ₁ $\delta\text{SiCl o.p.}$	130	134	<i>A</i> ₁ $\delta\text{SiCl o.p.}$	129
84	<i>E</i> δNSiCl	82	81	<i>E</i> δNSiCl	79

Frequencies are reported in units of cm^{-1} ; i.p. = in plane, o.p. = out of plane.TABLE 4. Vibrational spectrum of $\text{SiCl}_3\text{Br.NMe}_3^$

$\text{SiCl}_3\text{Br.N(CH}_3)_3^\dagger$		$\text{SiCl}_3\text{Br.N(CD}_3)_3^\dagger$	Calculated for C_{3v} symmetry		Assignment
Infrared	Raman	Raman	H9	D9	
<i>580vs</i>	<i>580vw</i> ‡ <i>570vw</i> ‡	<i>576vw</i> ‡ <i>567vw</i> ‡	636	635	<i>E</i> νSiCl
<i>537m</i>	<i>539w</i> <i>451w</i>	<i>452w</i>	572	542	<i>A</i> ₁ δNMe_3
<i>386s</i>	<i>384w</i>	<i>382w</i>	430	396	<i>E</i> $\delta\text{NMe}_3 + A_1\delta\text{N(CD}_3)_3$
<i>367s</i>	<i>369s</i> <i>342w</i>	<i>368s</i>	415	410	<i>A</i> ₁ νSiBr^\S
			372	370	<i>A</i> ₁ $\nu\text{SiCl}^\S + E\delta\text{N(CD}_3)_3$
<i>300ms</i>	<i>312w</i> <i>293w</i>	<i>326w</i> <i>290w br</i>			
	<i>228mw</i> <i>207m</i> <i>193w</i> <i>179ms</i> <i>161w</i>	<i>221mw</i> <i>209mw</i> <i>190w</i> <i>170ms</i>	248	230	<i>E</i> $\rho_r\text{NMe}_3$
	<i>103m</i> <i>96m</i>	<i>136w</i> <i>95m br</i>	166	165	<i>E</i>
			155	147	<i>A</i> ₁
			126	125	<i>E</i>
			132	122	<i>A</i> ₁
			70	68	<i>E</i>

*Frequencies reported in cm^{-1} .

†Metal-halogen skeletal stretching modes are in italics.

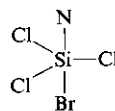
‡Split degeneracy in solid.

§Very mixed modes.

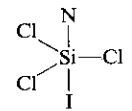
dal'' C_{3v} SiCl_3 residue in $[\text{SiCl}_3.\text{NMe}_3^+]$ are calculated to be in the range $500\text{--}460\text{ cm}^{-1}$ (c.f. ν_1 (507 cm^{-1}) and ν_3 (494 cm^{-1}) of PCl_3) considerably higher than the observed a_1 νSiCl frequency ($374\text{--}369\text{ cm}^{-1}$) which is more consistent with a "planar" SiCl_3 residue in a molecular adduct $\text{SiCl}_3\text{X.NMe}_3$; (iii) point (ii) would be further emphasized by the presence of a positive charge on the cation.

On the basis of the experimental data, a

molecular pentacoordinate (C_{3v}) formulation is preferred as shown below:



νSiCl 580 cm^{-1} *E*
 369 cm^{-1} *A*₁



νSiCl 605 cm^{-1} *E*
 374 cm^{-1} *A*₁

TABLE 5. Vibrational spectrum of $\text{SiCl}_3\text{I}\cdot\text{NMe}_3^*$

$\text{SiCl}_3\text{I}\cdot\text{N}(\text{CH}_3)_3^\dagger$		$\text{SiCl}_3\text{I}\cdot\text{N}(\text{CD}_3)_3^\dagger$ Raman	Calculated for C_{3v} symmetry		Approximate description of mode
Infrared	Raman		<i>H</i> 9	<i>D</i> 9	
<i>604s br</i>	<i>605vww</i> <i>544w</i>	<i>597w br</i> <i>464w br</i>	634 569	634 539	<i>E</i> νSiCl <i>A</i> ₁ δNMe_3 <i>A</i> ₁ $\delta\text{N}(\text{CD}_3)_3$
	<i>453w</i>	<i>393w</i>	430	396	<i>E</i> δNMe_3 <i>E</i> $\delta\text{N}(\text{CD}_3)_3$
<i>375w</i>	<i>374s</i>	<i>371mw</i>	365	362	<i>A</i> ₁ νSiCl
<i>334s</i>	<i>329ms</i>	<i>332s</i>	399	396	<i>A</i> ₁ $\nu\text{SiCl} + \nu\text{SiI}^\ddagger$
<i>281m</i>	<i>285vww</i>		247	232	<i>E</i> $\rho_r\text{NMe}_3$
<i>240w</i>		<i>235vw</i>			
<i>213mw</i>	<i>215ms</i>	<i>217w</i>	164	163	<i>E</i>
	<i>168ms</i>	<i>197mw</i>			
		<i>166ms</i>	142	134	<i>A</i> ₁
			118	118	<i>E</i>
	<i>109w</i>		101	101	<i>A</i> ₁
			66	64	<i>E</i>

*Frequencies are reported in units of cm^{-1} .

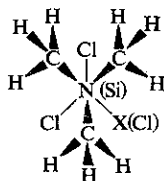
†Metal-halogen skeletal stretching modes are in italics.

‡Very mixed modes.

The calculations (Tables 4 and 5) give a very good match for C_{3v} symmetry, but a poor one for C_s . In the latter geometry, the bands were predicted to come at frequencies greater than 400 cm^{-1} as with the previous complexes, and very low force constants would have to be used to bring the frequencies down to 370 cm^{-1} .

Discussion

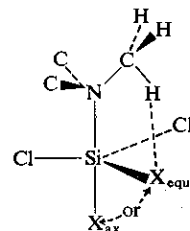
Having defined the configurations of the molecules $\text{SiCl}_3\text{X}\cdot\text{NMe}_3$, it is necessary to discuss the various factors which may influence the change in stereochemistry from C_s for $\text{X} = \text{H}$ or F to C_{3v} for $\text{X} = \text{Br}$ and I . It has been found that for trigonal bipyramidal trimethylamine complexes (5, 6, 10, 12), the bulky NMe_3 grouping adopts an axial staggered configuration with respect to the rest of the molecule. A staggered



configuration of the ligand would of course present the least amount of steric strain to the molecule.

An estimate of the degree of "ligand hydrogen - equatorial halogen" steric interaction (illustrated below) can be determined from a

molecular model of $\text{SiCl}_3\text{X}\cdot\text{NMe}_3$, based on a trigonal bipyramidal stereochemistry, having an axial staggered NMe_3 with respect to a coplanar arrangement of equatorial atoms. Placing the atom $\text{X} = \text{H}, \text{F}, \text{Cl}, \text{Br}$, or I in either the axial or equatorial sites, assuming tetrahedral angles at N and C and using single bond covalent radii, the maximum distances of $\text{H}\cdots\text{X}$ closest approach were calculated.

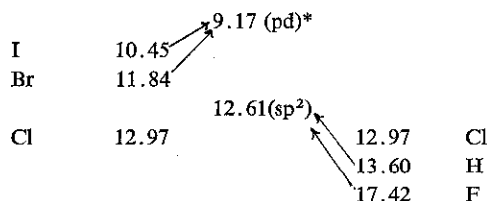


The computed $\text{H}\cdots\text{X}$ distances were all larger than a $\text{H}-\text{X}$ single bond distance although the bromide $\text{H}\cdots\text{Br}$ (2.46 Å) and iodide $\text{H}\cdots\text{I}$ (2.56 Å) distances were considerably shorter than the corresponding Van der Waal's distances, 3.15 and 3.35 Å respectively.

From simple steric arguments one would tend to favor equatorial H and F atoms but axial Br and I atoms which is in agreement with our experimental observations. It is perhaps interesting to note that intramolecular ligand hydrogen - equatorial fluorine ($\text{H}\cdots\text{F}$) hydrogen bonding would also probably favor an equatorial F atom in $\text{SiCl}_3\text{F}\cdot\text{NMe}_3$.

A semi-quantitative molecular orbital approach which can be considered when discussing the configurations of these trigonal bipyramidal molecules involves the energy gain on combining the orbitals of atom X and those of the central silicon atom. The sp^3d hybridized orbitals on the central atom of the trigonal bipyramidal molecule have been considered to be approximately divided into two orbital sets (7); axial linear pd hybrids and equatorial planar sp^2 hybrids. If the greatest energy to be gained by combining two orbitals occurs when the orbitals are evenly matched in energy, it is appropriate to consider as a first approximation the valence state ionization potentials (13) of the combining atom $X = H, F, Br,$ and I and compare them with the values for the pd axial and sp^2 equatorial orbitals on silicon shown in Scheme 1. This

Axial X I_v^X (eV) I_v^{Si} (eV) I_v^X (eV) Equatorial X



*In this approximation $E(pd) \approx E(p_z)$.

SCHEME 1

simple scheme predicts that equatorial H and F atoms and an axial I atom are energetically favored in $SiCl_3X.NMe_3$, which agrees with our experimental observation and favors the geometries predicted from simple steric arguments. Although the fate of bromine is not clear cut on this scheme, perhaps the steric effect of Br predominates to favor the axial position.

Normal Coordinate Analysis For $SiCl_3X.NMe_3$ in C_s and C_{3v} Symmetry

The bond lengths used are listed in Table 6; the equatorial bond length is taken as the SiX_4 length while the axial one is taken as being 5% longer, in anticipation of the weakness of the axial bond, and in accordance with the $AsCl_3.NMe_3$ and $GeCl_4.NMe_3$ X-ray data (10, 12). The silicon-nitrogen length is set at 2.01 Å. The methyl groups were treated as point masses. The internal and symmetry coordinates are shown in the appendix.

The force field for the calculations on $SiCl_3X.$

TABLE 6. Bond distances used in vibrational analysis

Bond	Distance (Å)
Si—N	2.01
N—Me	1.47
Si—H _{eq}	1.47
Si—H _{ax}	1.54
Si—F _{eq}	1.54
Si—F _{ax}	1.62
Si—Cl _{eq}	2.01
Si—Cl _{ax}	2.11
Si—Br _{eq}	2.28
Si—Br _{ax}	2.40
Si—I _{eq}	2.46
Si—I _{ax}	2.58

TABLE 7. Force constants for $SiCl_3X.NMe_3$ (C_{3v})

Force constant*	Value for X =			
	H	F	Br	I
f_R	2.70	2.70	2.70	2.70
f_D	1.35	3.05	0.98	0.70
f_a	1.20	1.20	1.20	1.20
f_{RR}	0.15	0.15	0.15	0.15
f_{RD}	0.15	0.15	0.15	0.15
f_α	0.489	0.489	0.489	0.489
f_β	0.648	0.665	0.669	0.642
f_γ	0.367	0.367	0.367	0.367
f_l	4.86	4.86	4.86	4.86
f_s	1.010	1.010	1.010	1.010
$f_{\gamma'}$	0.638	0.638	0.638	0.638
f_{is}	0.065	0.065	0.065	0.065

*In units of $mdyn/\text{Å}$, and $mdyn/rad$ or $mdyn \text{ Å}/rad^2$.

TABLE 8. Force constant* changes for $SiCl_3X.NMe_3$ (C_s)

X	f_R	f_r	f_D
H	2.70	1.35	2.70
F	2.70	1.35	6.11
Br	2.70	1.35	1.96
I	2.70	1.35	1.40

*In units of $mdyn/\text{Å}$, $mdyn/rad$, or $mdyn \text{ Å}/rad^2$.

NMe_3 was assumed to be roughly the same as the previously published $SiCl_4.NMe_3$. The equatorial stretching force constants were set equal to the parent SiX_4 stretching constants while the axial stretching constants were given half this value. The f_β in the C_{3v} configuration was the average of the $SiCl_4$ and SiX_4 angle bending force constants and varied for each X. The f_α was given the same value as the parent SiX_4 molecule, in this case, $SiCl_4$. The f_γ was set at 3/4 of the f_α . The stretching

force constant for the Si-N bond was arbitrarily set at 1.20 mdyn/Å. The actual numbers used in the C_{3v} calculations are shown in Table 7. Only the stretching force constants changed in going to C_s symmetry, and the changes are shown in Table 8. Interaction constants not listed, as well as torsional force constants, were set equal to zero.

Experimental

Trichlorosilane (from Matheson Co.) was purified by trap-to-trap distillation and outgassed at -78°C prior to use. Trichlorofluorosilane, trichlorobromosilane, and trichloroiodosilane were prepared by standard literature procedures (14-16) and purified by trap to trap distillation prior to use. The infrared and Raman spectra of the starting materials were found to be identical to those in the literature (17-18). Trimethylamine was dried and purified as described previously (19).

Dissociation pressure measurements have been reported for the systems $\text{SiCl}_3\text{H}/\text{NMe}_3$ and $\text{SiCl}_3\text{F}/\text{NMe}_3$ and clearly establish that only 1:1 complexes are capable of formation at low temperatures (1, 2). The $\text{SiCl}_3\text{I}\cdot\text{NMe}_3$ adduct prepared for the first time in this study proved to be the most stable of the series and could be analyzed directly from a vacuum ampoule by hydrolysis followed by conventional argentometric and pH titration techniques.

Anal. Calcd. for $\text{SiCl}_3\text{I}\cdot\text{NMe}_3$: Cl, 33.2; I, 39.6; $\text{Me}_3\text{N}:\text{Si} = 1$. Found: Cl, 33; I, 38.7; $\text{Me}_3\text{N}:\text{Si} = 1.10$.

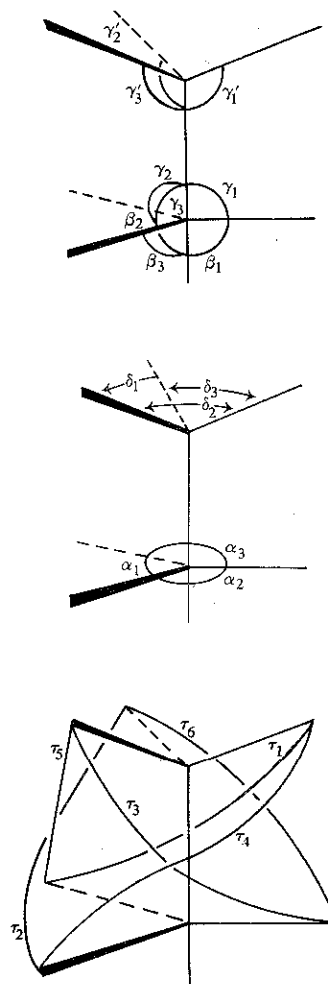
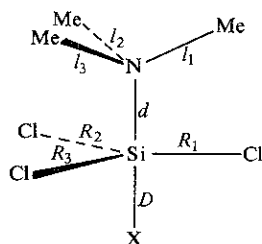
Vibrational spectra were recorded for thin films of the compounds formed by the slow deposition of a gaseous mixture of the appropriate halide with a slight excess of trimethylamine (approximately 1:1) onto the cold tip (-196°C) of a low temperature infrared or Raman cell.

The infrared spectra were recorded on a Beckman IR 11 and Perkin-Elmer 180 and 221 spectrometers. Raman spectra were recorded on a Spex 1401 spectrometer using krypton and argon ion laser excitation.

We wish to thank the National Research Council of Canada for financial support and for an NRCC scholarship (D.B.).

Appendix

C_{3v} Internal Coordinates



C_{3v} Symmetry Coordinates

Type A_1

$$\begin{aligned} S_1 &= (1/\sqrt{3})(\Delta R_1 + \Delta R_2 + \Delta R_3) \\ S_2 &= \Delta D \\ S_3 &= \Delta d \\ S_4 &= (1/\sqrt{3})(\Delta l_1 + \Delta l_2 + \Delta l_3) \\ S_5 &= (1/\sqrt{3})(\Delta \alpha_1 + \Delta \alpha_2 + \Delta \alpha_3) \\ S_6 &= (1/\sqrt{3})(\Delta \beta_1 + \Delta \beta_2 + \Delta \beta_3) \\ S_7 &= (1/\sqrt{3})(\Delta \gamma_1 + \Delta \gamma_2 + \Delta \gamma_3) \\ S_8 &= (1/\sqrt{3})(\Delta \gamma_1' + \Delta \gamma_2' + \Delta \gamma_3') \\ S_9 &= (1/\sqrt{3})(\Delta \delta_1 + \Delta \delta_2 + \Delta \delta_3) \\ S_{10} &= (1/\sqrt{6})(\Delta \tau_1 + \Delta \tau_2 + \Delta \tau_3 - \Delta \tau_4 \\ &\quad - \Delta \tau_5 - \Delta \tau_6) \end{aligned}$$

Type A_2

$$S_{11} = (1/\sqrt{6})(\Delta \tau_1 + \Delta \tau_2 + \Delta \tau_3 + \Delta \tau_4 + \Delta \tau_5 + \Delta \tau_6)$$

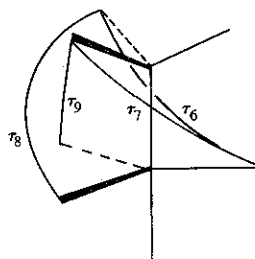
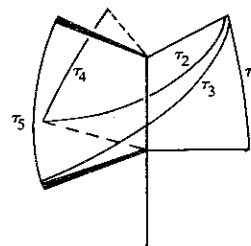
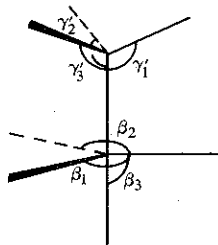
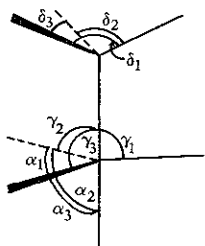
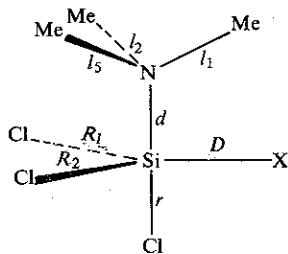
Type E_a

$$\begin{aligned}
 S_{12} &= (1/\sqrt{6})(2\Delta R_1 - \Delta R_2 - \Delta R_3) \\
 S_{13} &= (1/\sqrt{6})(2\Delta l_1 - \Delta l_2 - \Delta l_3) \\
 S_{14} &= (1/\sqrt{6})(2\Delta\alpha_1 - \Delta\alpha_2 - \Delta\alpha_3) \\
 S_{15} &= (1/\sqrt{6})(2\Delta\beta_1 - \Delta\beta_2 - \Delta\beta_3) \\
 S_{16} &= (1/\sqrt{6})(2\Delta\gamma_1 - \Delta\gamma_2 - \Delta\gamma_3) \\
 S_{17} &= (1/\sqrt{6})(2\Delta\gamma_1' - \Delta\gamma_2' - \Delta\gamma_3') \\
 S_{18} &= (1/\sqrt{6})(2\Delta\delta_1 - \Delta\delta_2 - \Delta\delta_3) \\
 S_{19} &= (1/2\sqrt{3})(2\Delta\tau_1 - \Delta\tau_2 - \Delta\tau_3 - 2\Delta\tau_4 \\
 &\quad + \Delta\tau_5 + \Delta\tau_6)
 \end{aligned}$$

$$S_{20} = (1/2)(\Delta\tau_2 - \Delta\tau_3 - \Delta\tau_5 + \Delta\tau_6)$$

Type E_b

$$\begin{aligned}
 S_{21} &= (1/\sqrt{2})(\Delta R_2 - \Delta R_3) \\
 S_{22} &= (1/\sqrt{2})(\Delta l_2 - \Delta l_3) \\
 S_{23} &= (1/\sqrt{2})(\Delta\alpha_2 - \Delta\alpha_3) \\
 S_{24} &= (1/\sqrt{2})(\Delta\beta_2 - \Delta\beta_3) \\
 S_{25} &= (1/\sqrt{2})(\Delta\gamma_2 - \Delta\gamma_3) \\
 S_{26} &= (1/\sqrt{2})(\Delta\gamma_2' - \Delta\gamma_3') \\
 S_{27} &= (1/\sqrt{2})(\Delta\delta_2 - \Delta\delta_3) \\
 S_{28} &= (1/2)(\Delta\tau_2 - \Delta\tau_3 + \Delta\tau_5 - \Delta\tau_6) \\
 S_{29} &= (1/2\sqrt{3})(2\Delta\tau_1 - \Delta\tau_2 - \Delta\tau_3 + 2\Delta\tau_4 \\
 &\quad - \Delta\tau_5 - \Delta\tau_6)
 \end{aligned}$$

 C_s Internal Coordinates C_s Symmetry CoordinatesType A'

$$\begin{aligned}
 S_1 &= \Delta D \\
 S_2 &= (1/\sqrt{2})(\Delta R_1 + \Delta R_2) \\
 S_3 &= \Delta r \\
 S_4 &= \Delta d \\
 S_5 &= \Delta l_1 \\
 S_6 &= (1/\sqrt{2})(\Delta l_2 + \Delta l_3) \\
 S_7 &= \Delta\alpha_1 \\
 S_8 &= (1/\sqrt{2})(\Delta\alpha_2 + \Delta\alpha_3) \\
 S_9 &= (1/\sqrt{2})(\Delta\beta_1 + \Delta\beta_2) \\
 S_{10} &= \Delta\beta_3 \\
 S_{11} &= \Delta\gamma_1 \\
 S_{12} &= (1/\sqrt{2})(\Delta\gamma_2 + \Delta\gamma_3) \\
 S_{13} &= \Delta\gamma_1' \\
 S_{14} &= (1/\sqrt{2})(\Delta\gamma_2' + \Delta\gamma_3') \\
 S_{15} &= (1/\sqrt{2})(\Delta\delta_1 + \Delta\delta_3) \\
 S_{16} &= \Delta\delta_3 \\
 S_{17} &= (1/\sqrt{2})(\Delta\tau_2 - \Delta\tau_3) \\
 S_{18} &= (1/\sqrt{2})(\Delta\tau_4 - \Delta\tau_5) \\
 S_{19} &= (1/\sqrt{2})(\Delta\tau_6 - \Delta\tau_7) \\
 S_{20} &= (1/\sqrt{2})(\Delta\tau_8 - \Delta\tau_9)
 \end{aligned}$$

Type A''

$$\begin{aligned}
 S_{21} &= (1/\sqrt{2})(\Delta R_1 - \Delta R_2) \\
 S_{22} &= (1/\sqrt{2})(\Delta l_2 - \Delta l_3) \\
 S_{23} &= (1/\sqrt{2})(\Delta\alpha_2 - \Delta\alpha_3) \\
 S_{24} &= (1/\sqrt{2})(\Delta\beta_1 - \Delta\beta_2) \\
 S_{25} &= (1/\sqrt{2})(\Delta\gamma_2 - \Delta\gamma_3) \\
 S_{26} &= (1/\sqrt{2})(\Delta\gamma_2' - \Delta\gamma_3') \\
 S_{27} &= (1/\sqrt{2})(\Delta\delta_1 - \Delta\delta_2) \\
 S_{28} &= \Delta\tau_1 \\
 S_{29} &= (1/\sqrt{2})(\Delta\tau_2 + \Delta\tau_3) \\
 S_{30} &= (1/\sqrt{2})(\Delta\tau_4 + \Delta\tau_5) \\
 S_{31} &= (1/\sqrt{2})(\Delta\tau_6 + \Delta\tau_7) \\
 S_{32} &= (1/\sqrt{2})(\Delta\tau_8 + \Delta\tau_9)
 \end{aligned}$$

1. A. B. BURG. *J. Am. Chem. Soc.* **76**, 2674 (1954).
2. J. E. FERGUSON, D. K. GRANT, H. H. HICKFORD, and C. J. WILKINS. *J. Chem. Soc.* **99** (1959).
3. H. J. CAMPBELL-FERGUSON and E. A. V. EBSWORTH. *J. Chem. Soc. (A)*, 1508 (1966).
4. H. J. CAMPBELL-FERGUSON and E. A. V. EBSWORTH. *J. Chem. Soc. (A)*, 705 (1967).
5. I. B. BEATTIE and G. A. OZIN. *J. Chem. Soc. (A)*, 542 (1969).
6. I. R. BEATTIE and G. A. OZIN. *J. Chem. Soc. (A)*, 2535 (1969).
7. E. L. MUETTERTIES, W. MAHLER, and R. SCHMUTZLER. *Inorg. Chem.* **2**, 613 (1963).
8. I. R. BEATTIE and G. A. OZIN. *J. Chem. Soc. (A)*, 370 (1970).
9. I. R. BEATTIE and T. R. GILSON. *J. Chem. Soc.* 6595 (1965).
10. M. S. BITTON and M. WEBSTER. *J. Chem. Soc. (A)*, 722 (1972).
11. I. R. BEATTIE and J. HORDER. *J. Chem. Soc. (A)*, 2655 (1969).
12. M. WEBSTER and S. KEATS. *J. Chem. Soc. (A)*, 836 (1971).
13. J. HINZE and H. H. JAFFÉ. *J. Am. Chem. Soc.* **84**, 540 (1962).
14. H. H. ANDERSON. *J. Am. Chem. Soc.* **72**, 2091 (1950).
15. W. C. SCHUMB and H. H. ANDERSON. *J. Am. Chem. Soc.* **59**, 651 (1937).
16. R. WEST and E. G. ROCHOW. *In Inorganic syntheses. Vol. 4. Edited by J. Bailar.* McGraw-Hill, New York, 1953, p. 41.
17. M-L. DELWAULLE. *J. Phys. Chem.* **56**, 355 (1952).
18. K. HAMADA, G. A. OZIN, and E. A. ROBINSON. *Can. J. Chem.* **49**, 477 (1971).
19. I. R. BEATTIE and G. A. OZIN. *J. Chem. Soc. (A)*, 2373 (1968).